

submitted to ApJ

Wavelet Band Powers of the Primordial Power Spectrum from CMB Data

Pia Mukherjee, Yun Wang

*Department of Physics & Astronomy, Univ. of Oklahoma, 440 W Brooks St., Norman, OK 73019
 email: pia@nhn.ou.edu, wang@nhn.ou.edu*

ABSTRACT

Measuring the primordial matter power spectrum is our primary means of probing unknown physics in the very early universe. We allow the primordial power spectrum to be an arbitrary function, and parametrize it in terms of wavelet band powers. Current cosmological data correspond to 11 such wavelet bands. We derive constraints on these band powers as well as H_0 , $\Omega_b h^2$ and $\Omega_m h^2$ from a likelihood analysis of current Cosmic Microwave Background Anisotropy (CMB) data using the Markov Chain Monte Carlo (MCMC) technique. Our results indicate a feature in the primordial power spectrum at $0.01 \lesssim k/(h^{-1}\text{Mpc}) \lesssim 0.1$, at a significance level of $\sim 1.5 \sigma$. MAP and Planck data should allow us to put tighter constraints on the primordial power spectrum.

1. Introduction

As a result of recent cosmological data, inflation (Guth 1981; Albrecht & Steinhardt 1982; Gott 1982; Linde 1983) has become increasingly well established as the plausible solution to the problems of standard cosmology (Kolb & Turner (1990); see Peebles & Ratra (2003) for a recent review). The primordial power spectrum is our primary window into unknown physics during inflation (Wang, Spergel, & Strauss 1999; Chung et al. 2000; Enqvist & Kurki-Suonio 2000; Lyth, Ungarelli, & Wands 2002). It is of critical importance that we try to extract the primordial power spectrum, $P_{in}(k)$, from observational data without assuming specific forms for it.

Cosmological parameters are being measured to impressive precision with the help of recent CMB and large scale structure (LSS) data. The parameter constraints thus deduced are however sensitive to assumptions regarding the power spectrum of primordial density perturbations. The primordial power spectrum is often assumed to be a power law, which represents many inflationary models (for example, see Linde (1983); Freese, Frieman, & Olinto (1990); La & Steinhardt (1991)). With such a parametrization the primordial power spectrum has been found to be scale invariant to a very good approximation, and its amplitude constrained (see for example Lewis & Bridle (2002)). However, there are many inflation models that predict primordial power spectra which cannot be parametrized by a simple power law (for example, Holman et al. (1991ab); Wang (1994); Randall,

Soljacic, & Guth (1996); Adams, Ross, & Sarkar (1997); Lesgourgues, Polarski, & Starobinsky (1997); Lesgourgues (2000)). These can represent unusual physics in the very early universe. For example, inflation might occur in multiple stages in effective theories with two scalar fields (Holman et al. 1991ab), or in a succession of short bursts due to symmetry breaking during an era of inflation in supergravity models (Adams, Ross, & Sarkar 1997).

With the quality of data improving, more attention is being paid to the nature of the primordial perturbations (for example, see Covi, Lyth, & Melchiorri (2002); Leach & Liddle (2002)). As more observational data become available, they increase our ability to probe the primordial power spectrum as an arbitrary function of scale. A model independent determination of the primordial power spectrum could uniquely probe physics of the very early universe, test what we have assumed about early universe physics, and provide powerful constraints on inflationary models. Wang, Spergel, & Strauss (1999) explored how this can be done with the CMB data from MAP¹ and LSS data from SDSS, using a piecewise constant function for $P_{in}(k)$. Wang & Mathews (2002) used the CMB data from Boomerang, Maxima, and DASI to place constraints on $P_{in}(k)$ (using linear interpolation to approximate the function between several k values equally spaced in $\log k$).

Here we employ wavelets in a model independent parametrization of the primordial power spectrum and obtain constraints from current CMB data. We use only CMB data here, but LSS (for example, see Hamilton & Tegmark (2002); Percival et al. (2002); Bahcall et al. (2003)), and CMB polarization (for example, see Kovac et al. (2002)) data can all be added to help break or reduce degeneracies between different cosmological parameters and help better constrain the primordial power spectrum.

We describe the wavelet parametrization of the primordial power spectrum in Sec.2. In Sec.3, we discuss the techniques that we have used to optimize our method. Sec.4 contains our results. Sec.5 contains a summary and discussions. Appendix A contains the details of the wavelet expansion.

2. Wavelet Band Powers of the Primordial Power Spectrum

Since the primordial matter density fluctuations form a homogeneous Gaussian random field, the wavelet band powers of the primordial power spectrum $P_{in}(k)$, can be written as (see Eq.(A11))

$$P_j = \frac{1}{2^j} \int_{-\infty}^{\infty} dk \left| \hat{\psi} \left(\frac{k}{2^j} \right) \right|^2 P_{in}(k), \quad (1)$$

where $\hat{\psi}$ is the Fourier transform of the wavelet ψ (see Appendix A). P_j 's represent a scale-by-scale band averaged Fourier power spectrum, where the banding is not arbitrary but well defined, and naturally adaptive (as wavelets by construction afford better k resolution at smaller k). The P_j 's

¹<http://map.gsfc.nasa.gov/>

are statistically independent by construction (see Appendix A and Fang & Feng (2000) for further discussion of these issues).

Figure 1 shows a primordial power spectrum with features (solid line), similar to that discussed by Elgaroy, Gramann, & Lahav (2002). The points are the wavelet band powers P_j , computed using Eq.(1). These P_j ’s can be thought of as being measured exactly from ideal data. Clearly, the wavelet band powers of the primordial power spectrum are excellent approximations of the primordial power spectrum at the central k values of the wavelet window functions, $\left| \hat{\psi} \left(\frac{k}{2^j} \right) \right|^2$ (dotted curves in Fig.1).

Hence we parametrize the primordial power spectrum $P_{in}(k)$ as follows [see Eq.(A12)]

$$P_{in}(k) = \sum_{j=0}^{\infty} P_j \left| \hat{\psi} \left(\frac{k}{2^j} \right) \right|^2. \quad (2)$$

The wavelet band powers P_j can be estimated from data that depend on the primordial power spectrum $P_{in}(k)$, for example, CMB and LSS data. We expect to estimate the wavelet band powers P_j with finite errors, which represent a measurement of the primordial power spectrum at the central k values of the wavelet window functions.

CMB data are in the form of band powers of the angular power spectrum C_l . We use these data to constrain cosmological parameters together with the wavelet band powers P_j . P_j ’s of unity corresponds to the default power of $A_s^2 = 2 \times 10^{-9}$ which is the level of power in modes larger and smaller than the covered range shown in Figure 1 (which is the entire range that the CMB and LSS data are sensitive to, including MAP and SDSS), and if all P_j ’s are set to unity we recover exactly the C_l spectrum that results from a scale invariant primordial power spectrum $P_s(k) = A_s^2 \left(\frac{k}{k_0} \right)^{n_s-1}$.

Figure 2 shows how each wavelet band window function, $\left| \hat{\psi} \left(\frac{k}{2^j} \right) \right|^2$ [shown in Figure 1], maps on to a window function in the CMB angular power spectrum multipole number l space, for one set of cosmological parameters. These window functions have been numbered 7 to 17, which correspond to a range in k of $0.0001 \lesssim k/(h \text{ Mpc}^{-1}) \lesssim 0.5$. The 11 band powers, P_7 through P_{17} (from small to large k), are sufficient to constrain the primordial power spectrum from current and near future cosmological data. The bands numbered 1 to 6 correspond to smaller k , bands numbered 18 and higher correspond to larger k ; the CMB data, upto an l_{max} of 1500, are insensitive to these bands, so that the corresponding band powers are not studied here [they are set to unity]. The solid curve is the CMB angular power spectrum C_l that includes contributions from all the P_j ’s [set to unity]. From Figure 2, and given that the data are band powers in C_l ’s, and each multipole l maps on to a range in k (for example, see Figure 4 of Tegmark, & Zaldarriaga (2002)) with dependence on cosmological parameters, we see that in constraining P_j using cosmological data some correlations between the P_j ’s will be introduced. The P_j ’s are also correlated somewhat with the cosmological parameters in ways that can be understood from Figure 2.

For comparison, instead of wavelet band powers, we can parametrize the primordial power spectrum as a continuous and arbitrary function determined by its amplitude at several wavenumbers,

equally spaced in $\log(k)$, using linear interpolation to approximate the function at intermediate wavenumbers. This is the method of Wang & Mathews (2002). In this work, we determine amplitudes at 11 wavenumbers corresponding to the central k values of the wavelet band powers. Figure 3 shows how each of these “binned” amplitudes map onto the CMB angular power spectrum multipole number l . The solid curve is the CMB angular power spectrum C_l with contributions from all the bins [all bin amplitudes set to 1]. The power in each bin, denoted here by a_j , is correlated with the power in neighbouring bins from the start, and ultimately the resulting correlations will be different from the wavelet banding method. The error bars on the estimates will also be correlated. See Wang & Mathews (2002) for further details about this method.

3. Optimization Techniques: Wavelet Projections and Markov Chain Monte Carlo

The usual approach to deriving cosmological constraints from CMB data is to grid over all the parameters being estimated and compute the likelihood at each point. Here, besides the 11 wavelet band powers (P_j ’s), we constrain H_0 , $\Omega_b h^2$ and $\Omega_c h^2$, assuming a flat- Λ universe and ignoring reionization and tensor modes. This results in 14 parameters. In order to place the most accurate and reliable constraint on the primordial power spectrum, we have chosen to compute the theoretical CMB angular power spectra at the accuracy of CMBFAST (Seljak & Zaldarriaga 1996) and CAMB (Lewis, Challinor, & Lasenby 2000). Our analysis would have been extremely time-consuming even on supercomputers. Fortunately, we are able to use two techniques which have made it possible for the analysis to be completed in a timely fashion.

First is the wavelet projections of the CMB angular power spectrum, C_l ’s. The CMB angular power spectrum has been expanded as follows

$$C_l(\mathbf{s}) = \sum_{j=0}^{\infty} P_j C_l^j(\mathbf{s}), \quad (3)$$

where \mathbf{s} represents the cosmological parameters other than the P_j ’s. We use CAMB² to compute the CMB angular power spectrum, in a form such that for given cosmological parameters other than the P_j ’s, the $C_l^j(\mathbf{s})$ are computed, so that there is no need to call CAMB when we vary the P_j ’s. This is significant since it saves computational time by many orders of magnitude. We expect this technique to be essential in constraining the primordial power spectrum with sufficient detail and speed.

The second technique is the Markov Chain Monte Carlo (MCMC) technique, illustrated for example in Lewis & Bridle (2002). The large number of parameters being varied here necessitates the use of this technique in the likelihood analysis. At its best, the MCMC method scales approximately linearly with the number of parameters. The method samples from the full posterior

²<http://camb.info/>

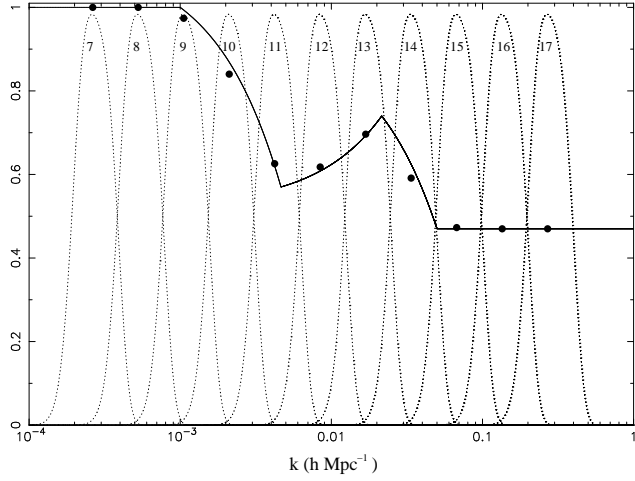


Fig. 1.— An example of a primordial power spectrum (solid line), and its wavelet band powers P_j s ($j=7,17$; points), together with the corresponding wavelet window functions (dotted lines). The y axis is in arbitrary units.

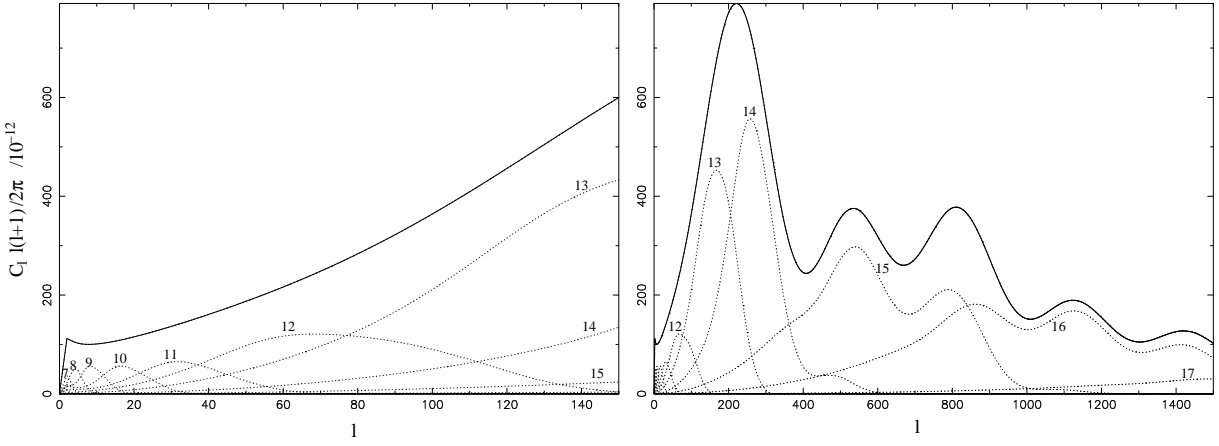


Fig. 2.— Mapping of the wavelet window functions of Figure 1 into window functions in the CMB multipole l space (dotted curves). The solid curve is the C_l spectrum that is the sum of contributions from all the wavelet bands (all the band powers, P_j , are set to unity here for illustration).

distribution of the parameters, and from these samples the marginalized posterior distributions of the parameters can be estimated. See Neil (1993) for a review, and Hannestad (2000); Knox et al. (2001); Rubino-Martin et al. (2002) for other applications of this method to CMB analysis. An MCMC sampler based on the Metropolis-Hastings algorithm has been made available in the software package CosmoMC (Lewis & Bridle 2002).

It would be interesting to include reionization and curvature, and obtain additional constraints from different kinds of LSS data and ultimately also CMB polarization. We defer such extensions to the near future.

4. Results

We use most of the recent high precision data for which experimental details are publically available. These are the latest Boomerang (Ruhl et al. 2002), Maxima (Lee et al. 2001), DASI (Halverson et al. 2002), VSA (Scott et al. 2002), CBI (Pearson et al. 2002) and Archeops (Benoit et al. 2002), together with COBE (Smoot et al. 1992).³ We use offset-lognormal band-powers (Bond et al. 2000) whenever available and marginalize over known calibration and beamwidth uncertainties. We estimate the wavelet band powers of the primordial power spectrum, as well as H_0 , $\Omega_b h^2$ and $\Omega_c h^2$.

All results shown in this paper are for the wavelet Daubachies 20 [see Appendix A].

For illustration, Figure 4(a) shows marginalized posterior distributions of the P_j ’s obtained at near currently popular values of H_0 , $\Omega_b h^2$ and $\Omega_c h^2$ of 68, 0.021 and 0.12 respectively. Since the P_j ’s are “fast” parameters for which we do not need to call CAMB (see Sec.3), this calculation takes of the order of 10 minutes on a Sparc Ultra Sun Workstation, to generate 10^5 MCMC samples. We find that the power in the 13th, 14th, 15th and 16th bands are best constrained and whilst the last three of these indicate slightly less power than unity, P_{12} has some indication of excess power though not at high significance.

Next, we fix the P_j ’s at unity and vary the three cosmological parameters; the resultant constraints are shown in Figure 4(b). This calculation takes much longer to compute than that for Figure 4(a). We allow $h = H_0/(100 \text{ kms}^{-1} \text{ Mpc}^{-1})$, $\Omega_b h^2$, and $\Omega_c h^2$ to vary between 0.4 and 1.0, 0.005 and 0.1, and 0.1 and 0.99 respectively. The marginalized parameter constraints are $h = 0.59 \pm 0.06$, $\Omega_b h^2 = 0.022 \pm 0.0015$ and $\Omega_c h^2 = 0.146 \pm 0.015$.

Finally, we allow all 14 parameters to vary and obtain Figure 5. We have used a weak age prior of $t_0 > 10$ Gyrs. All the P_j ’s are consistent with unity at 1.5σ . The cosmological parameters

³ACBAR results (Kuo et al. 2002) have not been included here as our numerical calculations were completed by the time the window functions became available.

are constrained to $h = 0.55 \pm 0.07$, $\Omega_b h^2 = 0.015 \pm 0.006$ and $\Omega_c h^2 = 0.145 \pm 0.026$.⁴⁵ Note that the derived value of the Hubble constant h is somewhat lower than the value of h derived assuming a scale-invariant primordial power spectrum, i.e., setting all the P_j s to unity. Figure 5 shows that current CMB data seem to favour a dip at a k of $\sim 0.01 h \text{ Mpc}^{-1}$ (from P_{12}) and excess power k of ~ 0.02 to $0.03 h \text{ Mpc}^{-1}$ (from P_{13} and P_{14}), followed by another small dip from P_{15} at k of $\sim 0.07 h \text{ Mpc}^{-1}$. Figure 6 shows the CMB power spectrum corresponding to the fitted cosmological parameters and P_j s and also the CMB power spectrum for the same cosmological parameters but with all P_j s set to unity. One can see where the P_j s are contributing. Most distinctly, by allowing the P_j s to vary, the CMB angular power spectrum receives significant positive contribution around the first peak and some negative contribution for the higher peaks.

The corresponding results for the case of the “binning” method are in Figure 7. Note that the primordial power spectrum reconstructed in this way shows similar features as the wavelet band powers of the primordial power spectrum [Figure 5]. This is reassuring since in the two methods the parameters being reconstructed have different correlations amongst themselves and with the other cosmological parameters [see Figures 2 and 3]. The bin amplitudes a_1 to a_6 seem to indicate the excess power at small k that was found by Wang & Mathews (2002). But from the marginalized distributions we see that these bin amplitudes are not satisfactorily constrained and vary over the entire range that was allowed in the runs. In comparison the wavelet banding method works better.

Now we examine the effect, on the wavelet band power results, of imposing statistical priors. If a Gaussian prior is introduced in the value of h , a weak conservative prior of 0.6 ± 0.1 (Branch 1998), together with the above mentioned weak age prior, what results is almost identical to Figure 5. If a stronger prior on h is introduced, that of $h = 0.72 \pm 0.08$ (Freedman et al. 2001), together with the BBN prior of 0.02 ± 0.002 (Burles, Nollett, & Turner 2001) for $\Omega_b h^2$, the constraints we get are $h = 0.65 \pm 0.07$, $\Omega_b h^2 = 0.02 \pm 0.002$ and $\Omega_c h^2 = 0.119 \pm 0.02$ and the significance of the feature reduces to under 1σ . Clearly, imposing the prior of a high Hubble constant tends to diminish the significance of the detected feature in the primordial power spectrum, as apparent in the Figure 3 of Wang & Mathews (2002). Without priors on the Hubble constant, the current CMB data seem to prefer a somewhat low Hubble constant of $h = 0.55 \pm 0.07$; it is not clear whether this is due to any systematic effects. Note that however, this lowish value of the Hubble constant is within the

⁴In this paper we quote the mean of the derived 1d distributions, instead of the maximum, for the constrained parameters, following Lewis & Bridle (2002). As discussed in Lewis & Bridle (2002), the MCMC samples from the posterior do not provide accurate estimates of parameter best-fit values, because in higher dimensions the best-fit region typically has a much higher likelihood than the mean but occupies a minuscule fraction of parameter space. Our main results are not affected by this.

⁵This corresponds to $\Omega_b = 0.048[0.023, 0.219]$ and $\Omega_c = 0.48[0.33, 0.96]$. Note the degeneracies between the cosmological parameters considered here. Due to the geometrical degeneracy, the location of the first acoustic peak nails the curvature of the universe (here taken to be zero) but a degeneracy between Ω_m and Ω_Λ , or equivalently Ω_m and h remains. The height of the first peak is degenerate for $\Omega_b h^2$ and $\Omega_c h^2$. Precise determination of the second and third peak heights can help determine $\Omega_b h^2$ and thus ease degeneracies (for example, see Efstathiou & Bond (1999); Hu et al. (2001); White & Cohn (2002)).

uncertainties of other independent measurements of H_0 (for example, see Branch (1998); Freedman et al. (2001); Gott et al. (2001); Saha et al. (2001)).

5. Discussion and Conclusions

In order to constrain unknown physics in the very early universe, it is important that we extract the primordial power spectrum $P_{in}(k)$ from observational data without assuming specific forms for it. We have used a wavelet band power expansion to extract $P_{in}(k)$ as a free function using recent high precision CMB data. The wavelet band powers of the primordial power spectrum are statistically independent by construction, and they are excellent approximations of the primordial power spectrum at the central k value of the wavelet window functions. The current CMB data correspond to 11 wavelet bands. We have measured the 11 wavelet band powers of the primordial power spectrum from current CMB data.

The wavelet band powers of $P_{in}(k)$ that we have extracted from current CMB data seems to indicate a feature in the primordial power spectrum at $0.01 \lesssim k/(h \text{ Mpc}^{-1}) \lesssim 0.1$, at a significance level of $\sim 1.5 \sigma$. The binning cum linear interpolation approach of Wang & Mathews (2002) yields an estimated $P_{in}(k)$ with a similar feature at roughly the same location in k with comparable significance. Our results are consistent with previous work by Wang & Mathews (2002). MAP and Planck⁶ data should allow us to put a tighter constraint on the primordial power spectrum (Lesgourgues, Prunet, & Polarski 1999; Wang, Spergel, & Strauss 1999; Hannestad 2001; Matsumiya, Misao Sasaki, & Yokoyama 2002; Tegmark, & Zaldarriaga 2002).

We note that several other groups have studied the constraint on specific types of features of the primordial power spectrum from current observational data; our findings are consistent with these results (Silk, & Gawiser 2000; Atrio-Barandela et al. 2001; Barriga et al. 2001; Hannestad, Hansen, & Villante 2001; Elgaroy, Gramann, & Lahav 2002).

The advantage of our approach in this paper versus previous work is as follows. We parametrize the primordial power spectrum by its wavelet band powers P_j . Wang, Spergel, & Strauss (1999) parametrize the primordial power spectrum by a step function [i.e., top-hat banding]; this leads to an estimated primordial power spectrum $P_{in}(k)$ that is *discontinuous*, while the $P_{in}(k)$ estimated using wavelet band powers is *continuous*. Wang & Mathews (2002) used linear interpolation of $P_{in}(k)$ values at several k values [equally spaced in $\log k$]; this lead to a continuous estimated $P_{in}(k)$, but the $P_{in}(k)$ values estimated from data are correlated, while the wavelet band powers P_j are statistically independent by construction [see Eqs.(1)(2)].

Finally we note that by computing the wavelet projections of C_l [see Eq.(3)] for each set of cosmological parameters excluding the P_j 's, we avoid computing C_l when we vary the wavelet band

⁶<http://astro.estec.esa.nl/Planck/>

powers P_j in the likelihood analysis, which leads to an improvement in speed of many orders of magnitude. This, together with the MCMC technique, made it possible for us to estimate all the 11 relevant wavelet band powers from the current CMB data in a timely fashion. We expect that our method will be efficient in yielding tighter and detailed constraints on $P_{in}(k)$ when applied to MAP and Planck data.

We acknowledge the use of CAMB and CosmoMC. This work was supported by NSF CAREER grant AST-0094335 at the Univ. of Oklahoma.

REFERENCES

Adams, J.A., Ross, G.G., & Sarkar, S. 1997, Nuclear Physics B, 503, 405

Albrecht, A., Steinhardt, P. J. 1982, Phys. Rev. Lett., 48, 1220

Atrio-Barandela, F., Einasto, J., Müller, V., Mücket, J. P., & Starobinsky, A. A. 2001, ApJ, 559, 1

Bahcall, N.A. et al. 2003, ApJ, in press, astro-ph/0205490

Barriga, J., Gaztanaga, E., Santos, M., & Sarkar, S. 2001, MNRAS, 324, 977

Benoit, A., et al. 2002, submitted to A&A Letter, astro-ph/0210305

Bond, J.R., Jaffe, A.H., & Knox, L.E. 2000, ApJ, 533, 19

Branch, D. 1998, ARA&A, 36, 17

Burles, S., Nollett, K.M., & Turner, M.S. 2001, ApJ, 552, 1

Chung, D.J.H., Kolb, E.W., Riotto, A., & Tkachev, I.I. 2000, Phys. Rev. D, 62, 043508

Covi, L., Lyth, D.H., Melchiorri, A. 2002, hep-ph/0210395

Efstathiou, G., & Bond, J. R. 1999, MNRAS, 304, 75

Elgaroy, O.; Gramann, M.; Lahav, O. 2002 MNRAS, 333, 93

Enqvist, K.; Kurki-Suonio, H. 2000, Phys. Rev. D, 61, 043002

Fang, L.Z., & Feng, L.L. 2000, ApJ, 539, 5

Freedman, W. L. et al. 2001, ApJ, 553, 47

Freese, K., Frieman, J.A., & Olinto, A.V. 1990, Phys. Rev. Lett., 65, 3233

Gott, J. R. 1982, Nature, 295, 304

Gott, J. R., Vogeley, M. S., Podariu, S., Ratra, B. 2001, ApJ, 549, 1

Guth, A.H. 1981, Phys. Rev. D, 23, 347

Halverson, N.W., et al. 2002, ApJ, 568, 38

Hamilton, A.J.S., Tegmark, M. 2002, MNRAS, 330, 506

Hannestad, S. 2001, Phys.Rev. D, 63, 043009

Hannestad, S, Hansen, S.H., & Villante, F.L. 2001, Astropart.Phys. 16, 137

Hannestad, S. 2000, Phys. Rev. D61, 023002

Holman, R., Kolb, E.W., Vadas, S.L., & Wang, Y. 1991a, Phys. Rev., D43, 3833

Holman, R., Kolb, E.W., Vadas, S.L., & Wang, Y. 1991b, Phys. Lett., B269, 252

Hu, W., Fukugita, M., Zaldarriaga, M., & Tegmark, M. 2001, ApJ, 549, 669

Jungman, G., Kamionkowski, M., & Kosowsky, A.; Spergel, D.N. 1996, Phys. Rev. D54, 1332

Knox, L., Christensen, N., & Skordis, C. 2001, ApJ, 563, L95

Kolb, E.W., & Turner, M.S. 1990, *The Early Universe* (Addison-Wesley Publishing Company)

Kovac, J. et al. 2002, astro-ph/0209478

Kuo, C.L., et al. 2002, submitted to ApJ, astro-ph/0212289

La, D., & Steinhardt, P.J. 1991, Phys. Rev. Lett., 62, 376

Leach, S.M., & Liddle, A.R. 2002, astro-ph/0207213

Lee, A.T., et al. 2001, ApJ, 561, L1

Lesgourgues, J., Polarski, D., & Starobinsky, A.A. 1997, Nuclear Physics B, 497, 479

Lesgourgues, J., Prunet, S., & Polarski, D. 1999, MNRAS, 303, 45

Lesgourgues, J. 2000, Nucl. Phys. B582, 593

Lewis, A., Challinor, A., & Lasenby, A. 2000, ApJ, 538, 473, astro-ph/9911177

Lewis, A., & Bridle, S. 2002, astro-ph/0205436

Linde, A.D. 1983, Phys. Lett., 129B, 177

Lyth, D. H., Ungarelli, C., & Wands, D. 2002, Phys. Rev. D, in press, astro-ph/0208055

Matsumiya, M.; Sasaki, M.; Yokoyama, J. 2002, Phys.Rev. D, 65, 083007

Mukherjee, P., Hobson, M., & Lasenby, A. 2000, MNRAS, 318, 1157

Neil, R.M. 1993, <ftp://ftp.cs.utoronto.ca/pub/radford/review.ps.gz>

Pearson, T.J., et al. 2002, submitted to ApJ, astro-ph/0205388

Peebles, P.J.E., & Ratra, B. 2003, RMP, in press, astro-ph/0207347

Percival, W.J. et al. 2002, MNRAS, in press, astro-ph/0206256

Randall, L., Soljacic, M., & Guth, A. 1996, Nucl. Phys. B472, 377

Rubino-Martin, J.A., et al. 2002, submitted to MNRAS, astro-ph/0205367

Ruhl, J.E., et al. 2002, astro-ph/0212229

Saha, A. et al. 2001, ApJ, 562, 314

Schwarz, D.J., Terrero-Escalante, C.A., & Garcia, A.A. 2001, Phys. Lett. B, 517, 243

Scott, P.F., et al. 2002, astro-ph/0205380

Seljak, U., & Zaldarriaga, M. 1996, ApJ, 469, 437

Silk, J., & Gawiser, E. 2000, Physica Scripta T85, 132 (2000)

Smoot, G.F., et al. 1992, ApJ, 396, L1

Tegmark, M., & Zaldarriaga, M. 2002, Phys. Rev. D, 66, 103508

Wang, Y. 1994, Phys. Rev., D50, 6135

Wang, Y., Spergel, D.N., & Strauss, M.A. 1999, ApJ, 510, 20

Wang, Y., & Mathews, G.J. 2001, ApJ, 573, 1

White, M., & Cohn, J.D. 2002, AmJPh, 70, 106

A. Wavelet Band Powers

We now describe our parametrization of the primordial power spectrum using wavelets.

The wavelet transform bases are obtained from dilations and translations of a certain (mother) function $\psi(x)$ via

$$\psi_{j,l}(x) = \left(\frac{2^j}{L}\right)^{1/2} \psi(2^j x/L - l). \quad (\text{A1})$$

where $\psi(x)$ is in general real, defined on the interval $[0, 1]$, and obeys several restrictive mathematical relations first derived by Daubechies (1992) in order for the resulting wavelet basis to be discrete, orthogonal and compactly-supported. These are the kind of wavelets we consider here. j and l are scale and position indices respectively, and the wavelet bases are orthogonal with respect to both these indices,

$$\int_{-\infty}^{\infty} \psi_{j,l}(x) \psi_{j',l'}(x) dx = \delta_{jj'} \delta_{ll'}.$$

A periodic function $f(x)$ of period L , sampled at 2^J equally spaced points between 0 and L , can be expanded in terms of the wavelet basis as

$$f(x_i) = \sum_{j=0}^{J-1} \sum_{l=0}^{2^j-1} b_{j,l} \psi_{j,l}(x_i), \quad (\text{A2})$$

where the coefficients $b_{j,l}$ are given by

$$b_{j,l} = \int_0^L f(x) \psi_{j,l}(x) dx. \quad (\text{A3})$$

The scale index j increases from 0 to $J - 1$, and the wavelets with increasing j represent the structure in the function on increasingly smaller scales, with each scale a factor of 2 finer than the previous one. The index l (which runs from 0 to $2^j - 1$) denotes the position of the wavelet $\psi_{j,l}$ within the j th scale. Thus $b_{j,l}$ measures the signal in $f(x)$ on scale $L/2^j$, and centred at position $lL/2^j$ in physical space and centred at wavenumber $2\pi \times 2^j/L$ in Fourier space.

The Fourier decomposition of function $f(x)$ is given by

$$f(x) = \sum_{n=-\infty}^{\infty} \epsilon_n e^{i2\pi nx/L} \quad (\text{A4})$$

and the Fourier coefficient ϵ_n is

$$\epsilon_n = \frac{1}{L} \int_0^L f(x) e^{-i2\pi nx/L} dx. \quad (\text{A5})$$

Since both the discrete wavelet transform (DWT) and the Fourier transform (FT) bases are complete, there exists a relationship between the Fourier and wavelet coefficients. Substituting equation (A4) in (A3) gives

$$b_{j,l} = \sum_{n=-\infty}^{\infty} \epsilon_n \hat{\psi}_{j,l}(-n), \quad (\text{A6})$$

and similarly equations (A5) and (A2) give

$$\epsilon_n = \frac{1}{L} \sum_{j=0}^{\infty} \sum_{l=0}^{2^j-1} b_{j,l} \hat{\psi}_{j,l}(n), \quad (\text{A7})$$

where $\hat{\psi}_{j,l}(n)$ is the FT of the wavelet $\psi_{j,l}$ and is related to the FT of the basic wavelet (using (A1)) by

$$\hat{\psi}_{j,l}(n) = \int_0^L \psi_{j,l}(x) e^{-i2\pi nx/L} dx = \left(\frac{2^j}{L}\right)^{-1/2} \hat{\psi}\left(\frac{n}{2^j}\right) e^{-i2\pi nl/2^j}. \quad (\text{A8})$$

For a homogeneous random Gaussian field the one point distribution of the $b_{j,l}$ with respect to the index l is Gaussian for every j and the distributions of $b_{j,l}$ and $b_{j+1,l'}$ are uncorrelated (there exist no scale-scale correlations, of any order, as defined for example in Mukherjee, Hobson & Lasenby (2000)). Hence

$$\langle b_{j,l}, b_{j',l'} \rangle = P_j \delta_{j,j'} \delta_{l,l'} \quad (\text{A9})$$

implying that the DWT covariance matrix is j -diagonal. $P_j = \frac{1}{L} \sum_{l=0}^{2^j-1} |b_{j,l}|^2$ is the power of perturbations in wavelet coefficients of scale j .⁷ Correspondingly, the Fourier amplitudes ($|\epsilon_n|$) of such a field have a Gaussian one point distribution and their phases are random, so that

$$\langle \epsilon_n, \epsilon_{n'} \rangle = P(n) \delta_{n,n'}. \quad (\text{A10})$$

Let us note that (A9) is a stronger statement than (A10).⁸ Using these relations the wavelet and Fourier power spectra can be related as

$$P_j = \frac{1}{2^j} \sum_{n=-\infty}^{\infty} \left| \hat{\psi}\left(\frac{n}{2^j}\right) \right|^2 P(n). \quad (\text{A11})$$

It can be seen that P_j is a band averaged Fourier power spectrum, from which one can attempt to reconstruct the Fourier power spectrum in the following way:

$$\hat{P}(n) = \sum_{j=0}^{\infty} P_j \left| \hat{\psi}\left(\frac{n}{2^j}\right) \right|^2. \quad (\text{A12})$$

⁷When the random field is ergodic, the 2^j coefficients at a given scale can be taken as 2^j independent measurements. The average over 1 is thus a fair estimation of the ensemble average.

⁸This is because non-Gaussianity in Fourier space may be obscured by the central limit theorem. The non-Gaussianity should still be detected in wavelet space, due to the simultaneous scale and position localization property of the wavelet bases.

In order to parametrize the primordial power spectrum in a model independent way, we need to estimate the power in certain bands in k . The bands should be logarithmically spaced in k , as in Wang & Mathews (2002). To find a unique number for the appropriate number of bands to use, we adopt the DWT approach to banding. While in the Fourier approach the phase space is split such that the resolution in wavenumber k is highest at all k ($\Delta k \rightarrow 0$), and the resolution in position x is lowest, ($\Delta x \rightarrow \infty$), in the wavelet approach these resolutions are adaptive, so that an optimal chopping of the phase space is achieved whilst satisfying the uncertainty relation $\Delta x \Delta k \geq 2\pi$ (see Fang & Feng (2000) for a discussion). Wavelets afford good k resolution at small k and poorer resolution by factors of 2 as j (or position resolution) increases. Further, the wavelet band powers P_j , for a Gaussian random field, are statistically independent by definition, and one cannot have more independent bands (Fang & Feng 2000). Equations (A11) and (A12) show how the primordial Fourier power spectrum can be parametrized in terms of P_j 's which represent a scale-by-scale band-averaged Fourier power spectrum with \log_2 spacing.

All results shown in this paper are for the wavelet Daubachies 20. We have also studied the case for the Symmlet 8 wavelet, obtaining very similar results. The larger the number associated with the wavelet, the more smooth is the wavelet in real space, and the lesser their compact support in real space (less localized, though compact support is technically more involved a concept than localization, and while wavelets can be localized in both real and Fourier space, it is impossible for a function to have compact support in both spaces). For our purpose, since we hope to be able to pick up sharp features in the primordial (Fourier) power spectrum, wavelets that are smooth in real space are preferable. In fact wavelets that have compact support in Fourier space rather than in real space (often called band-limited wavelets) should do better. Examples of such wavelets are the Shannon wavelet and the Meyer wavelet. We defer their use for a future paper as these are less frequently used wavelets so that the relevant software is not easily available.

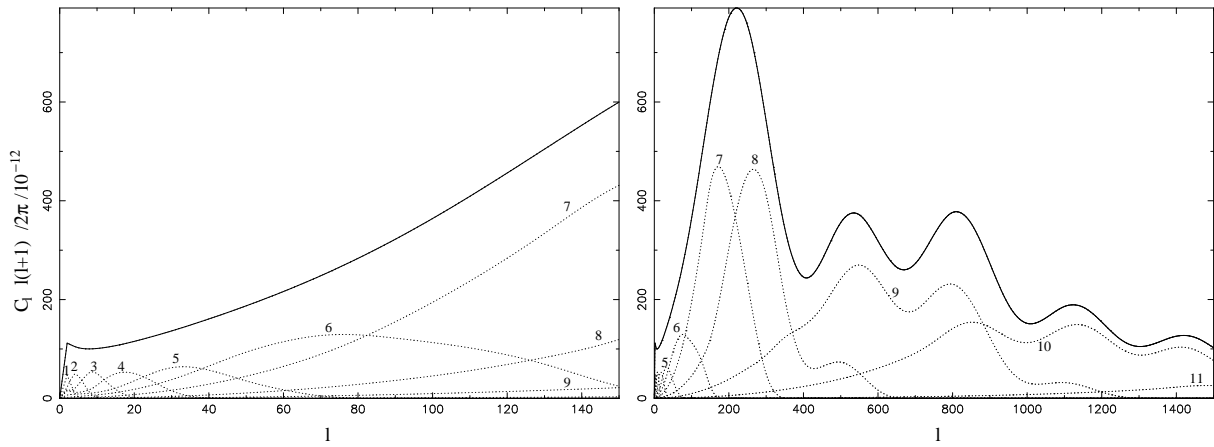


Fig. 3.— Mapping of an arbitrary number of bins, here chosen to be 11, to correspond exactly to the central k values of the 11 wavelet bands discussed above, into window functions in the CMB multipole l space (dotted curves). The solid line is the C_l spectrum that includes contributions from all the bins (all the bin amplitudes are set to unity here for illustration).

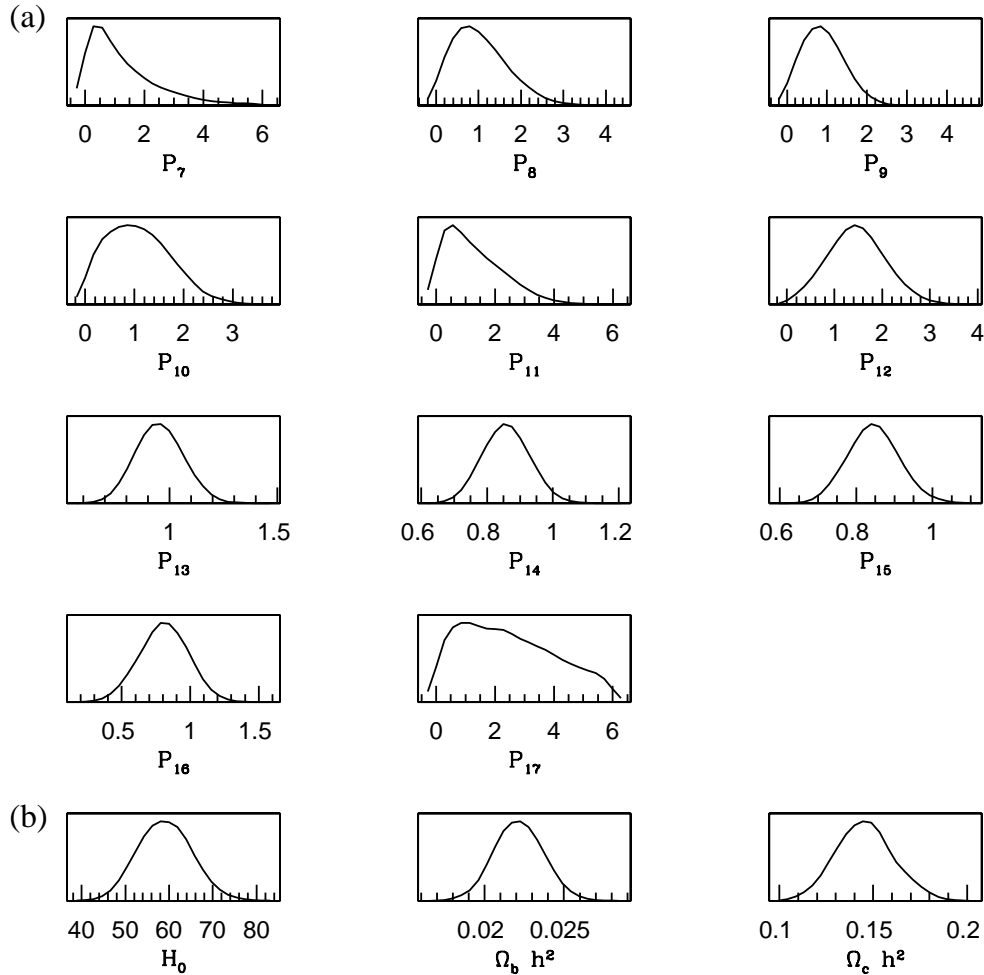


Fig. 4.— (a) The 1d marginalized posterior distributions of the 11 wavelet band powers (P_j s; $j=7,17$) at the near favoured values of the cosmological parameters. (b) The 1d marginalized posterior distributions of the 3 cosmological parameters we vary here at P_j s of unity (i.e. with a scale invariant primordial power spectrum).

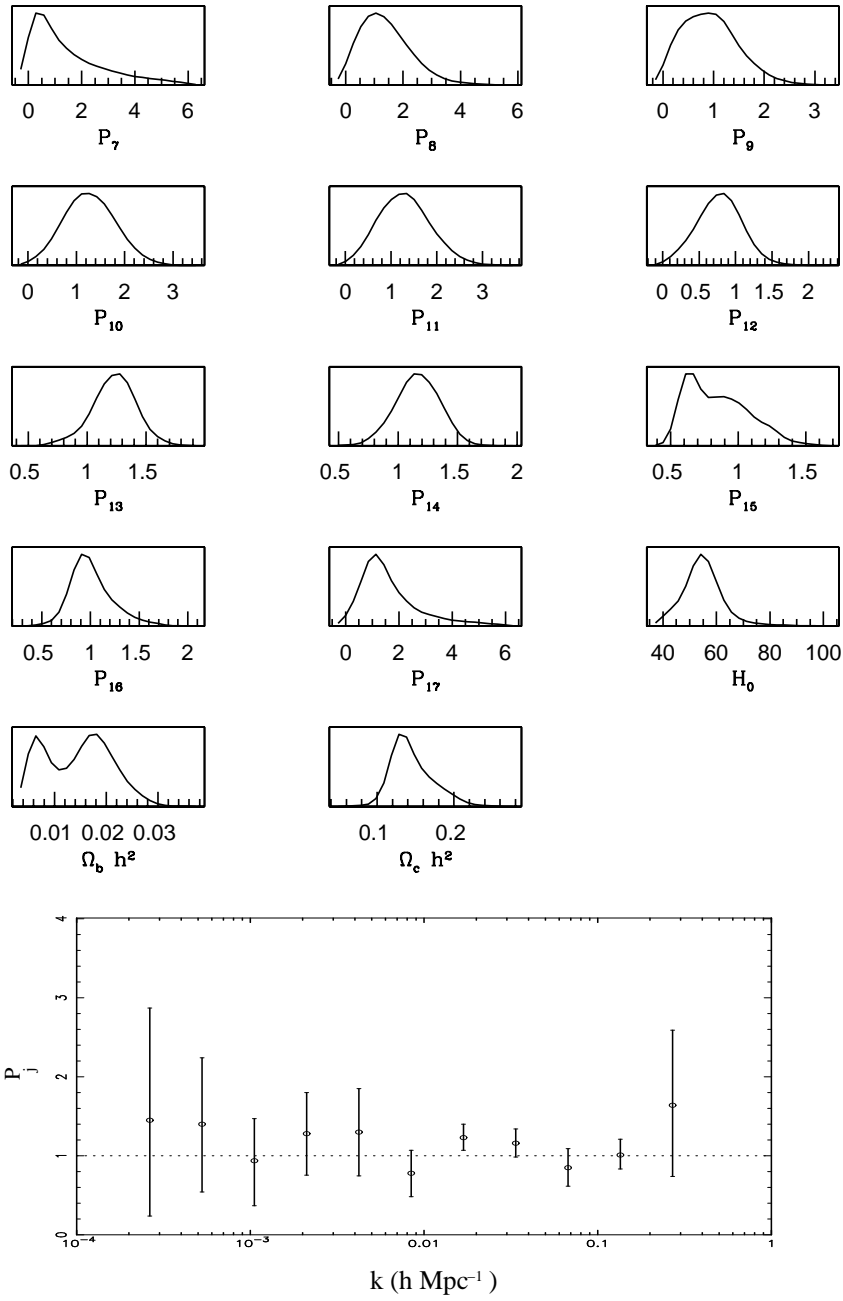


Fig. 5.— The 1d marginalized posterior distributions obtained upon varying all the 14 parameters. The bottom plot shows the constrained P_j s ($j=7,17$) versus scale.

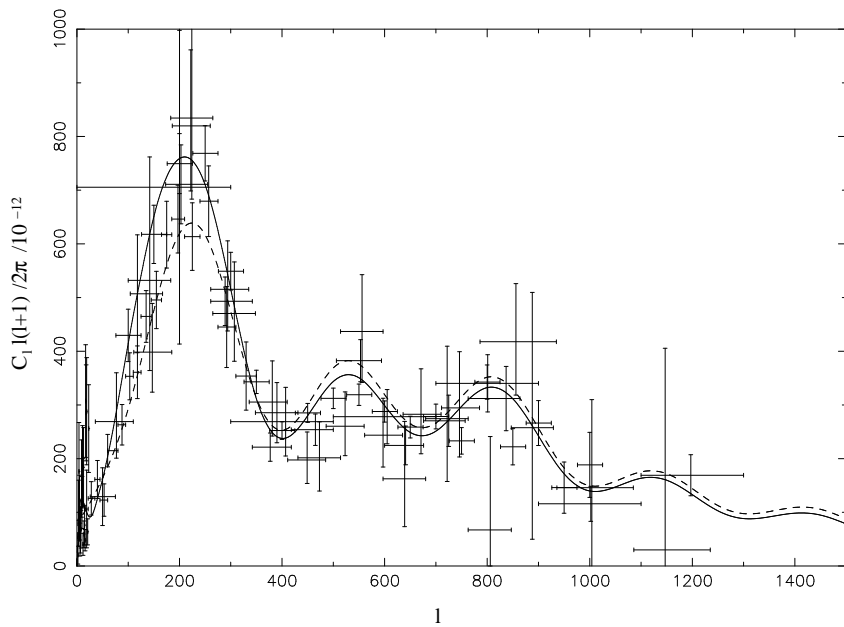


Fig. 6.— The solid line shows the CMB power spectrum at fitted values of the cosmological parameters and P_{js} s. The dashed line shows the CMB power spectrum for the same cosmological parameters at P_{js} s of unity. All the data points considered in the analysis are plotted. The error bars do not include calibration and beamwidth uncertainties.

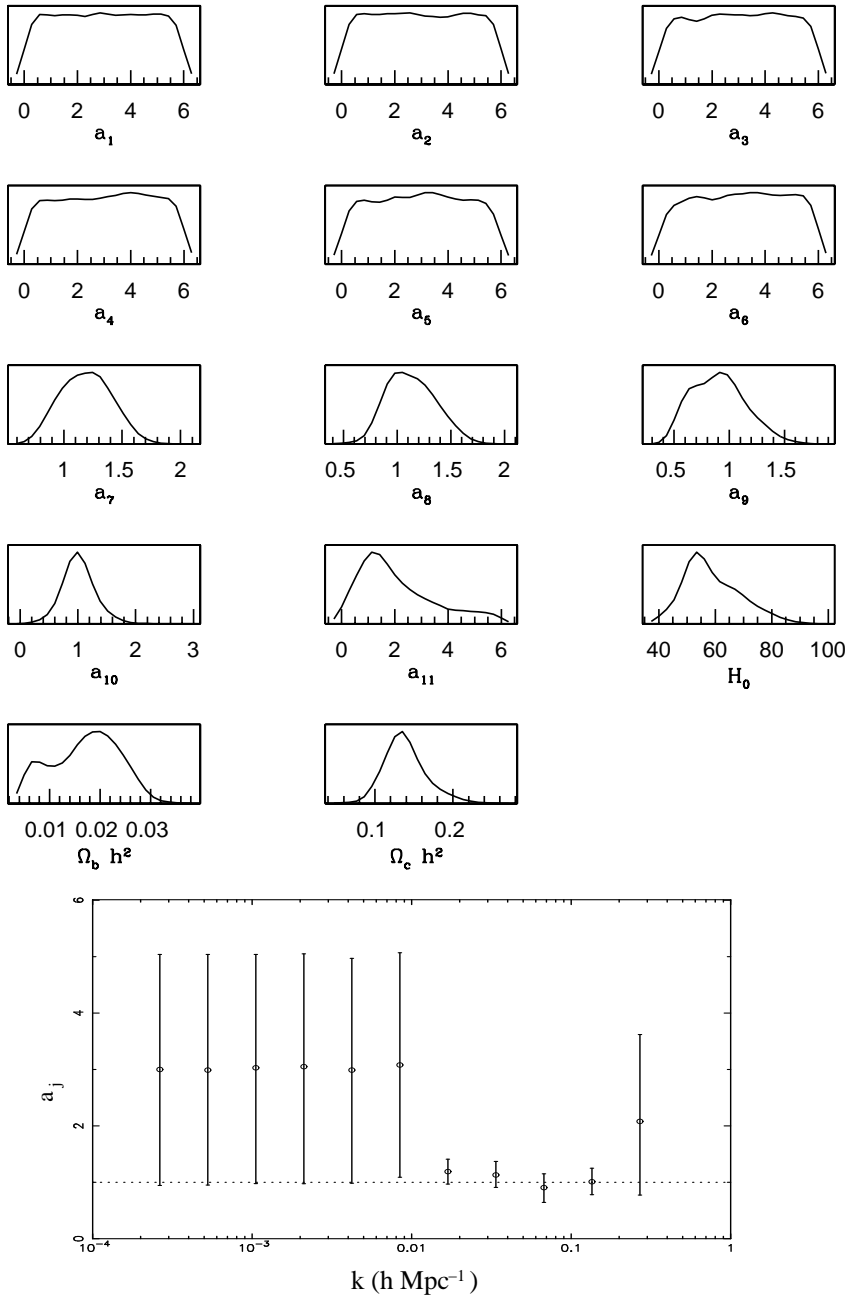


Fig. 7.— Results obtained by parameterizing the primordial power spectrum with bin amplitudes a_j s in 11 bins ($j=1,11$) corresponding exactly to the central k values of the wavelet bands.